Australian National University
NATURAM PRIMUM COGNOSCERE RERUM

CAASTRO
ARC CENTRE OF EXCELLENCE
FOR ALL-SKY ASTROPHYSICS

HI gas measurements of field galaxies at z~0.1 & 0.2 using HI spectral stacking technique

Jonghwan Rhee (RSAA, ANU & CAASTRO)

Martin A. Zwaan, Frank H. Briggs, Jayaram N. Chengalur, Philip Lah,
Tom Oosterloo, and Thijs van der Hulst

OUTLINE

- Why care about H I?
- H I spectral Stacking technique
- Measuring H I gas content at z~0.1 and 0.2
- Cosmic H I gas evolution

HI gas in the Universe

- Tentative reservoir of star formation fuel
- Structure & Kinematics of galaxies
- Tracer of Dark matter potential
- Characterize EoR / Dark age

H I gas in higher redshift

- Knowledge of H I gas is limited to nearby universe
- Different technique adopted at $z > 2.0$ (DLA)
- At intermediate redshift $0.2 < z < 2.0$, DLA can be observed only from space.

Why Hard to Detect H I 21cm line z > 0.1

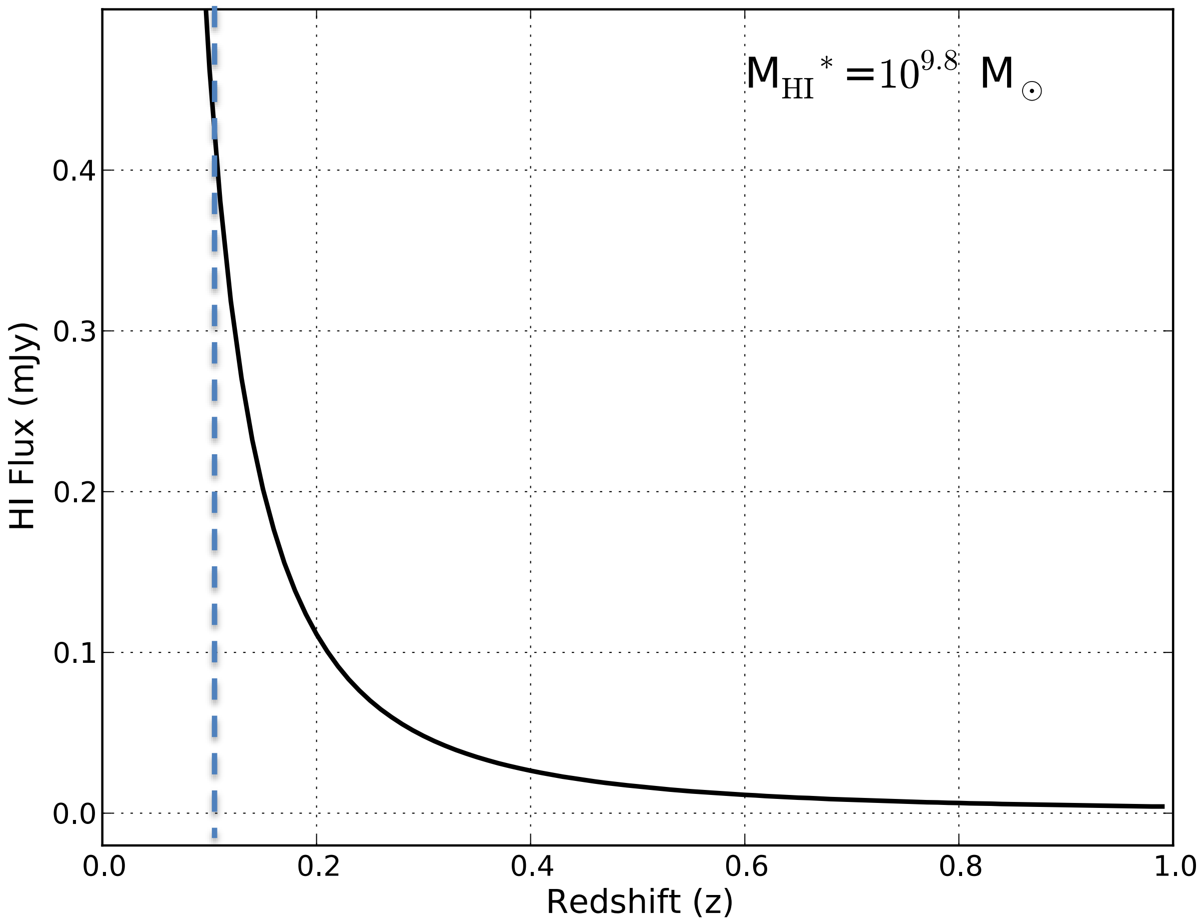

HI detection beyond z~0.1

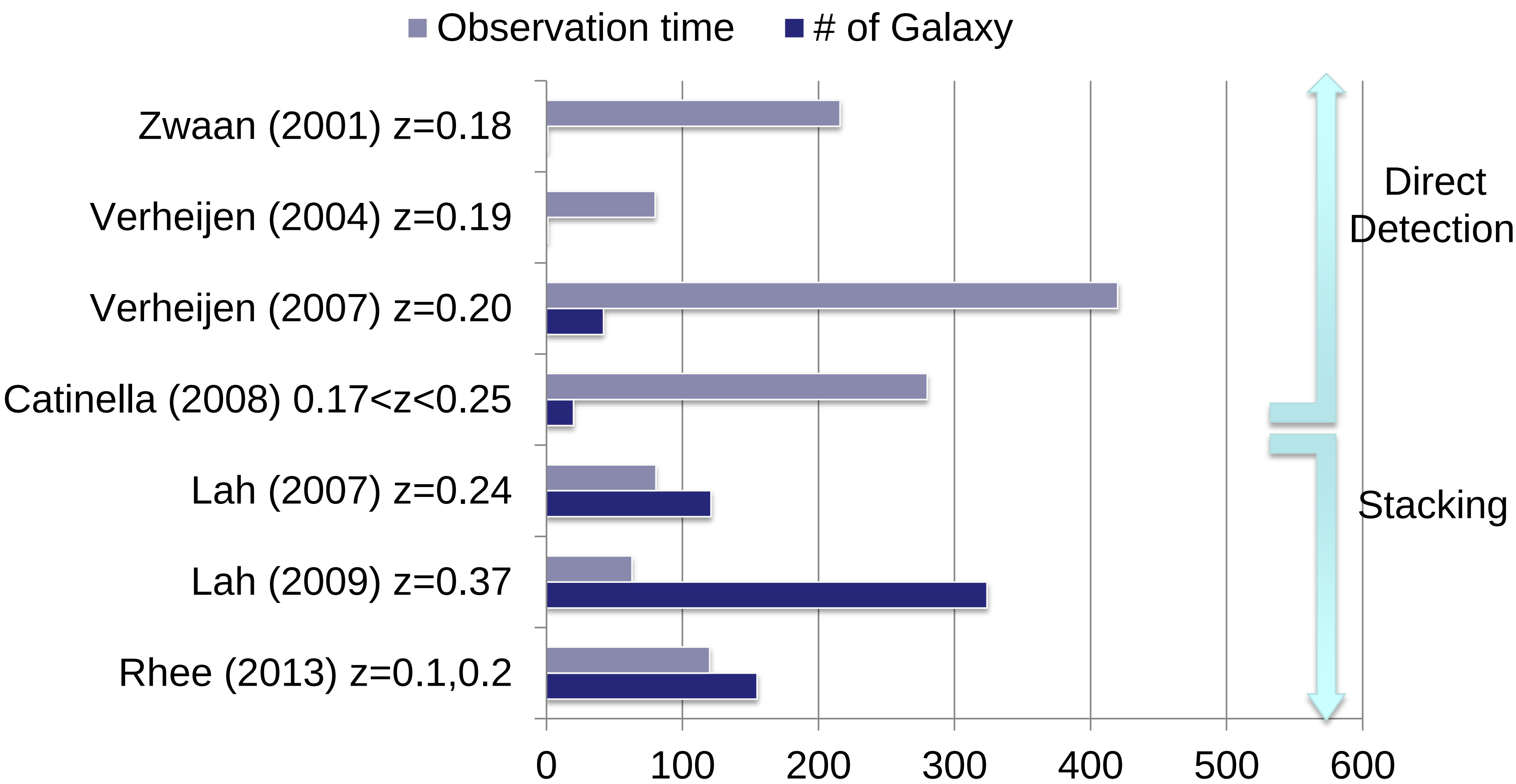

Spectral Signal Stacking

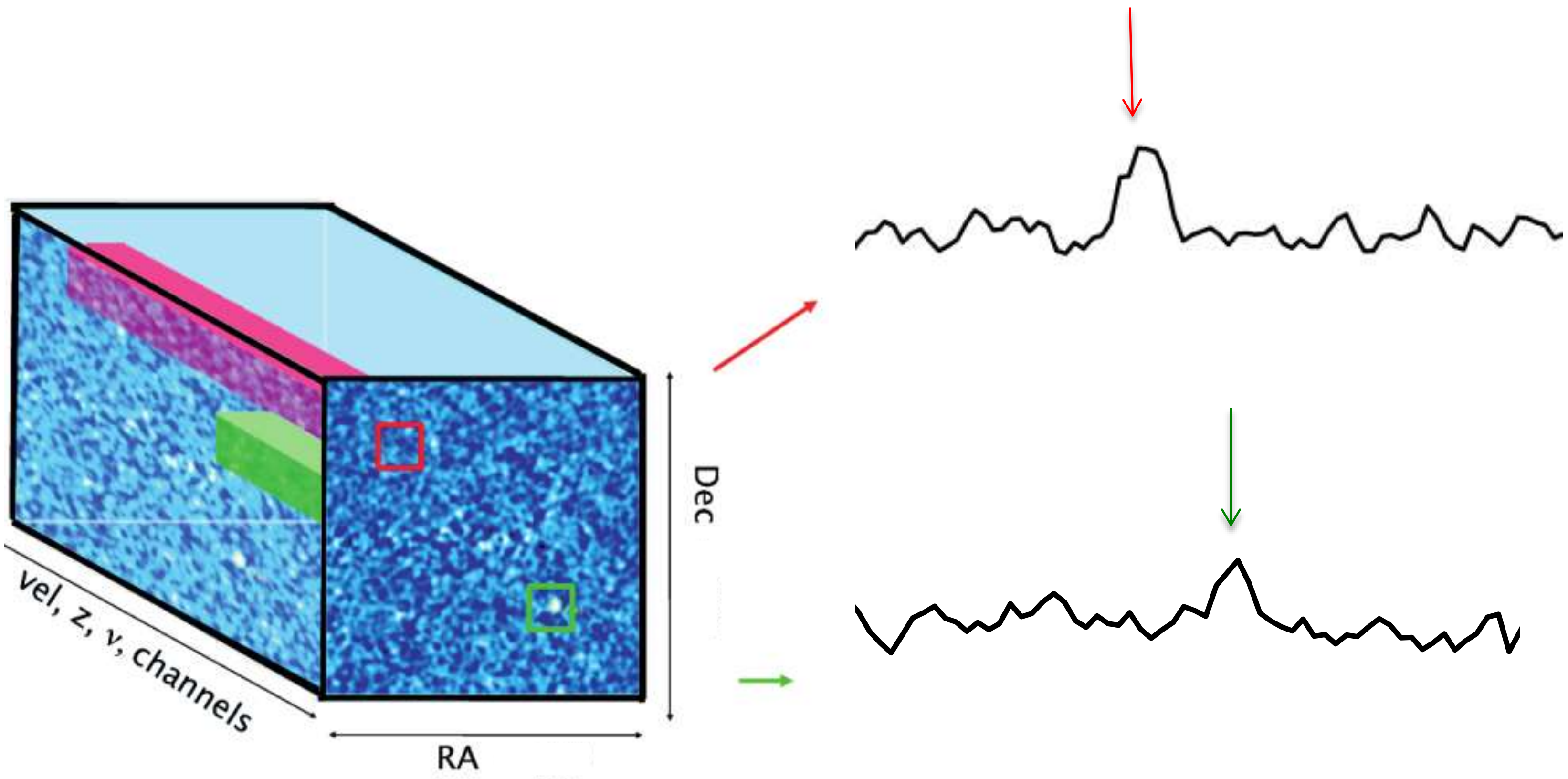

CNOC2 0920+37 Field

- One of the fields taken by the Second Canadian Network for Observational Cosmology (CNOC2) Field Galaxy Redshifts Survey.
- Positions, redshifts, UBVRI photometry for 1630 galaxies.
- Only 155 galaxies lie within the WSRT frequency and beam coverage(1 deg).

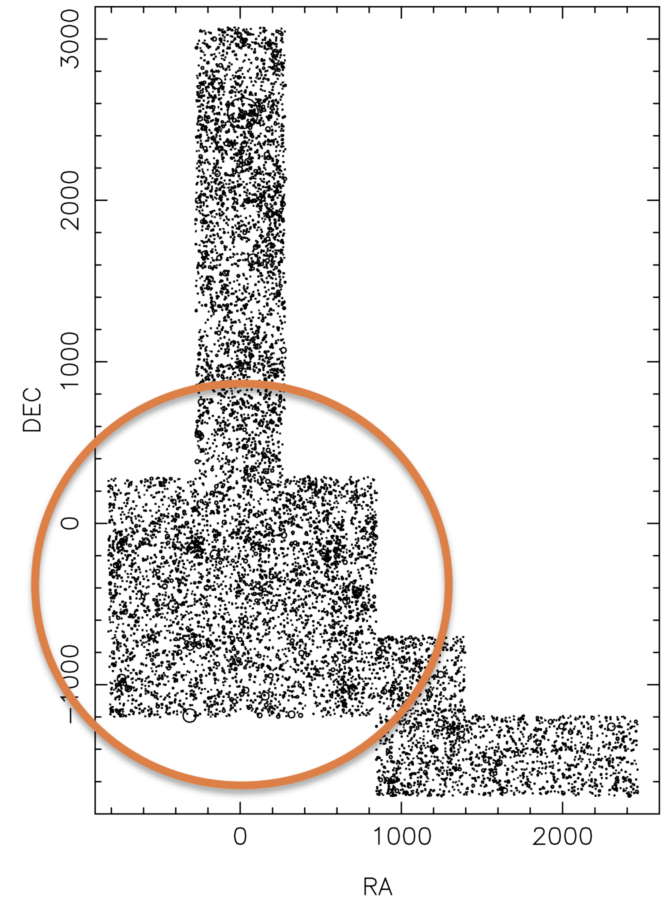

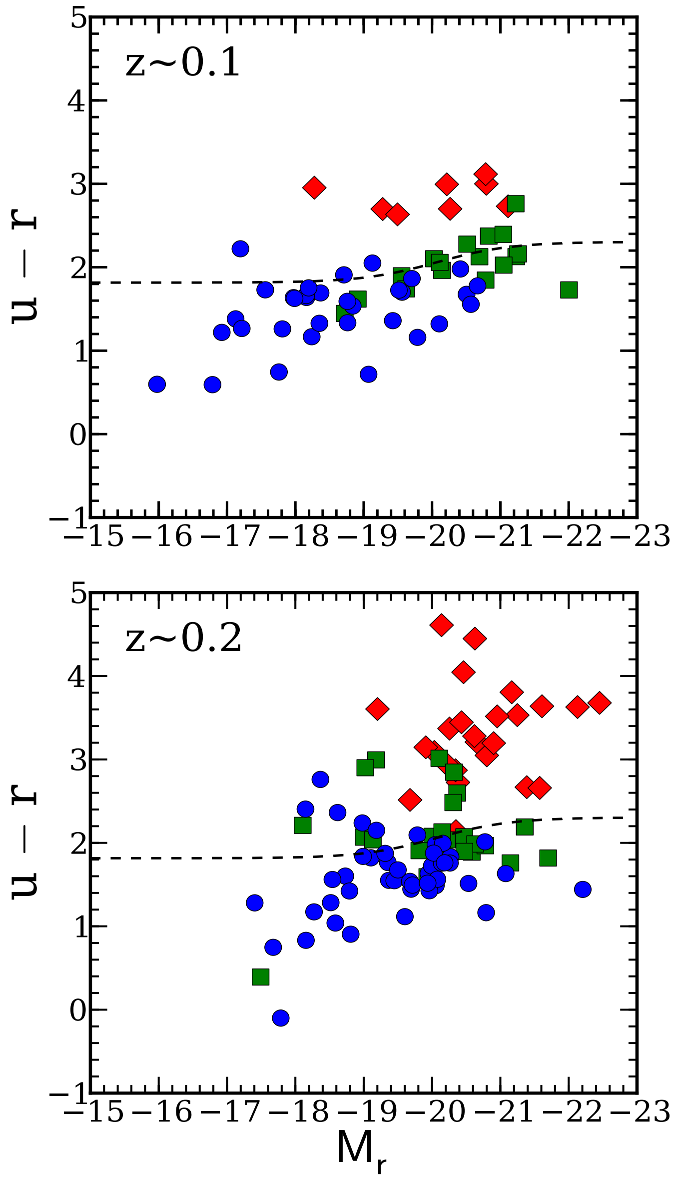

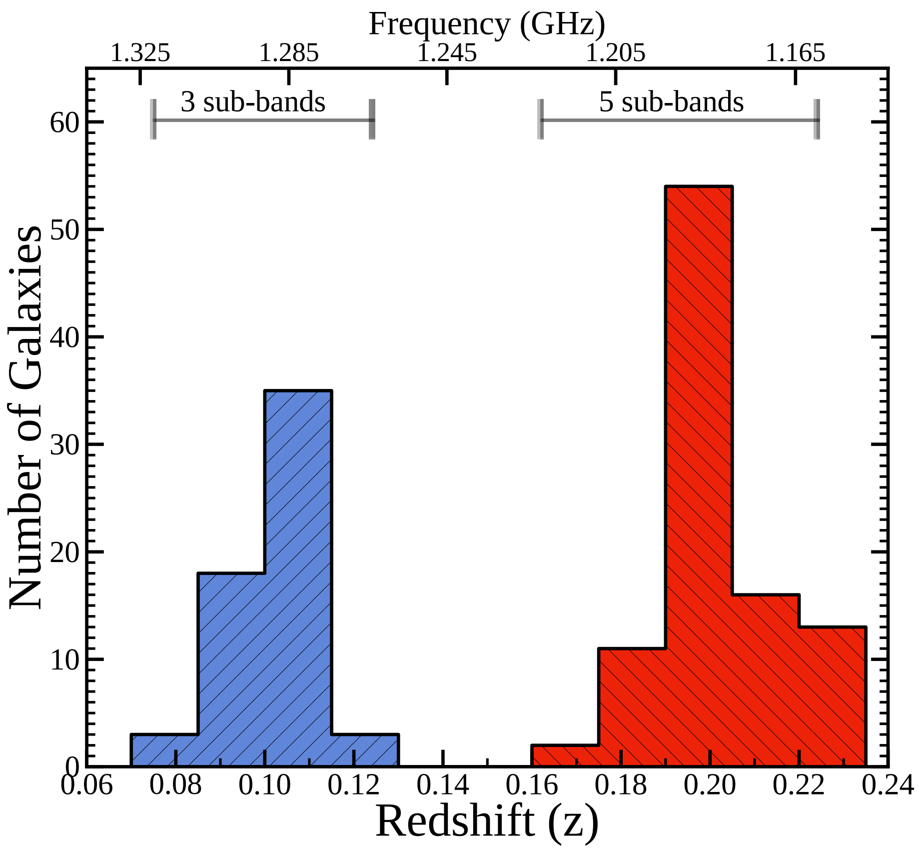

- Among a total of 155 galaxies,
  59 galaxies at z~0.1, 96 galaxies at z~0.2

WSRT observation

- 12 hr x 10 days in 2003
- A total of on-source integration time of ~106 hr
- Observation Frequency

  - 1160 ~ 1321 MHz (0.075 < z <0.224)
  - 8 x 20 MHz BW / 128 channels per band
  - 156.25 kHz (37.9 km/s) channel width
- **AIPS** and **CASA** used for data reduction

  (flagging, calibration, self-calibration, peeling, imaging)

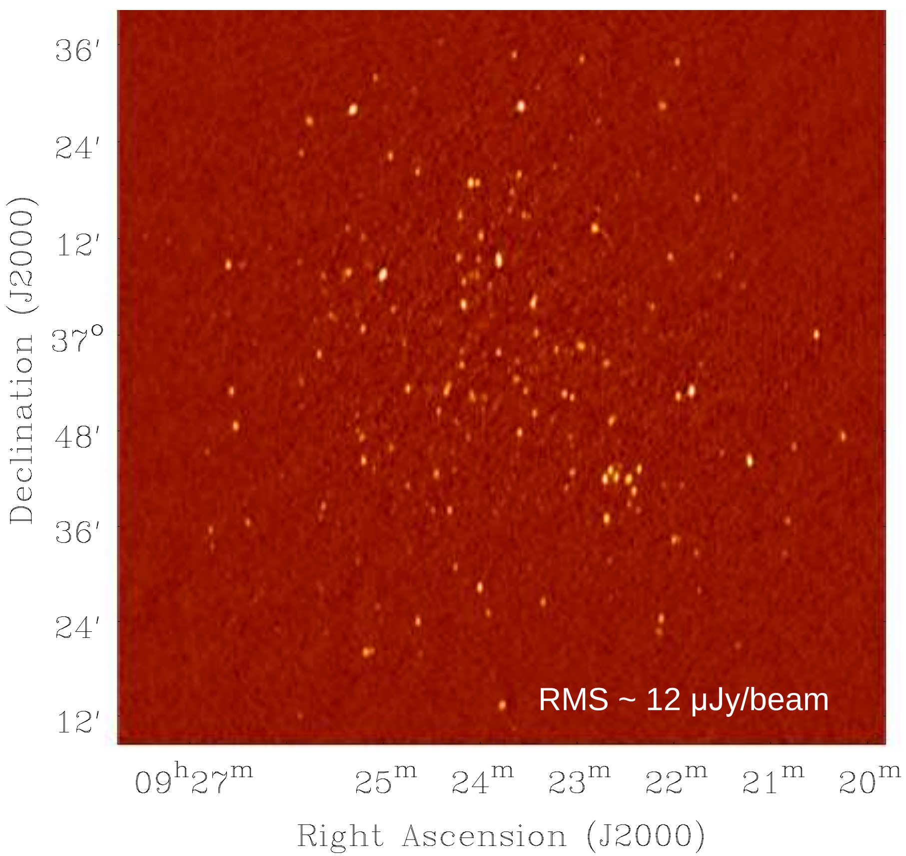

Continuum map at z~0.1

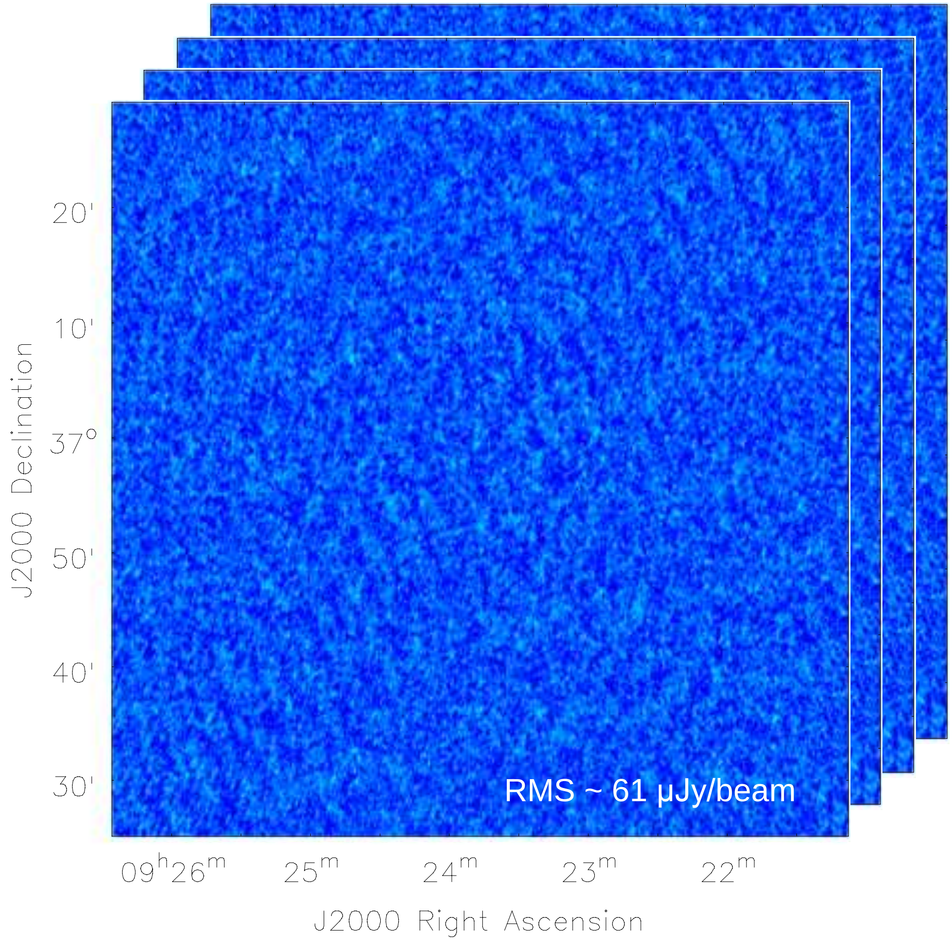

Line data cube of a sub-band

Direct Detection

- Implementing a source finding software, **DUCHAMP,** with data cubes.
- Cross-checking CNOC2 catalogue and optical images from SDSS
- 11 objects found at z~0.1,
  2 objects found at z~0.2

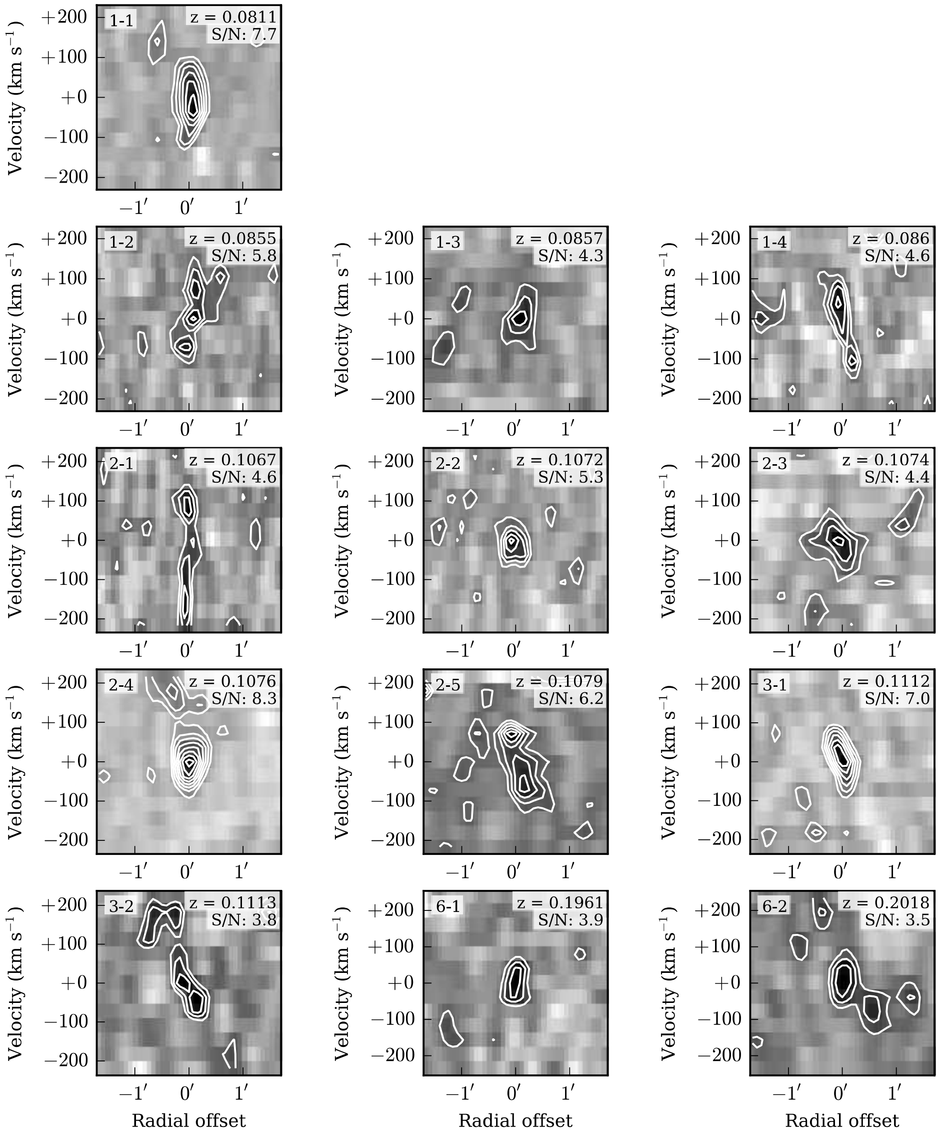

Galaxy HI-optical size

- WSRT synthesized beam

~33 arcsec x 20 arcsec

(~50 kpc x 31 kpc @ z~0.1)

- Used relation between HI size and optical size (SDSS petrosian radius) from Broeils & Rhee (1997)

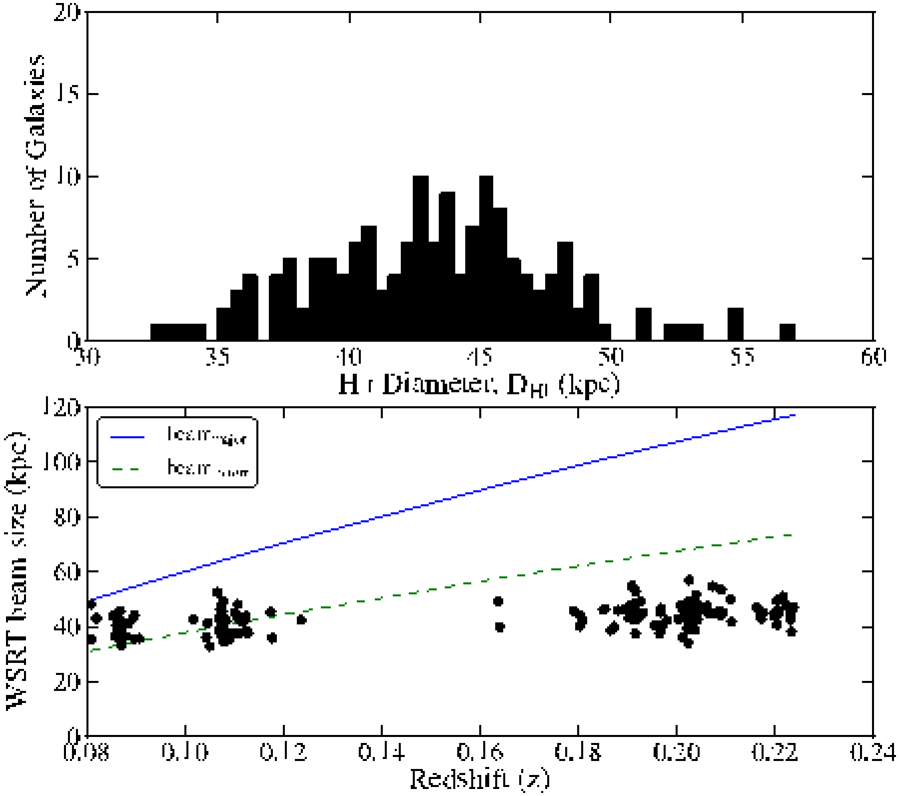

HI stacking

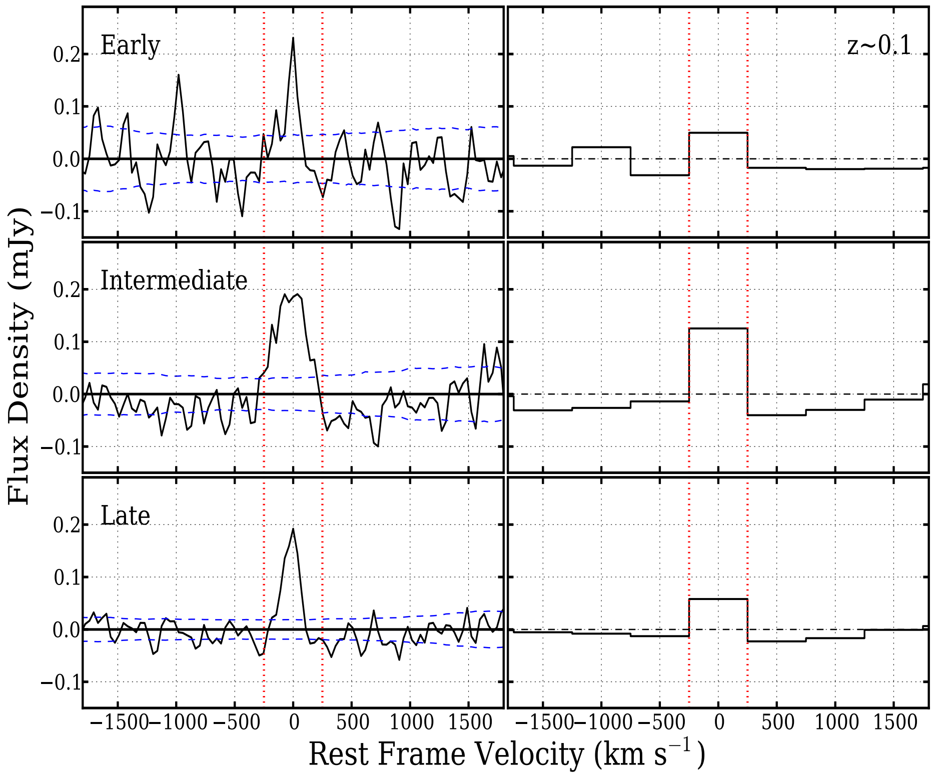

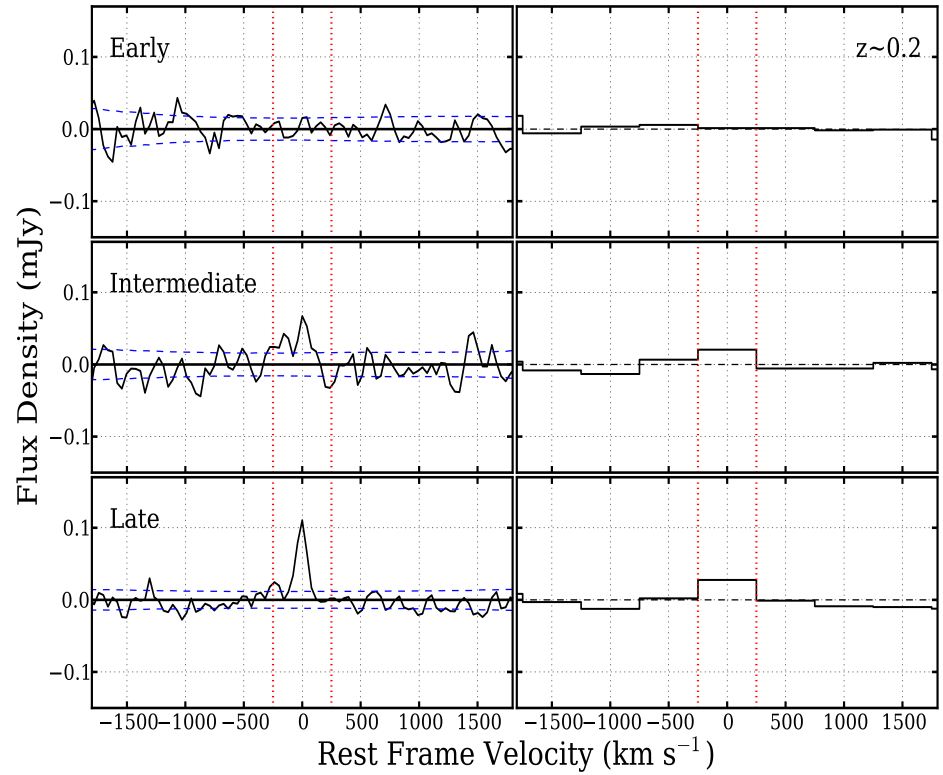

$$S_{average} = \frac{\sum_i w_i' S_i'}{\sum_i w_i'}, \qquad w_i' = \frac{1}{\sigma_i'^2}$$

$$\frac{M_{HI}}{M_\odot} = \frac{236}{(1+z)} \left(\frac{D_L}{\mathrm{Mpc}}\right)^2 \left(\frac{\int S_V\, dV}{\mathrm{mJy\ km\ s^{-1}}}\right)$$

H I mass density

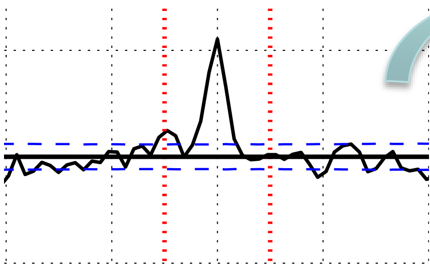

$$\rho_{\mathrm{H\,I}} = \frac{\sum M_{\mathrm{H\,I}}}{\sum L_B} \times \rho_{L_B(z)},$$

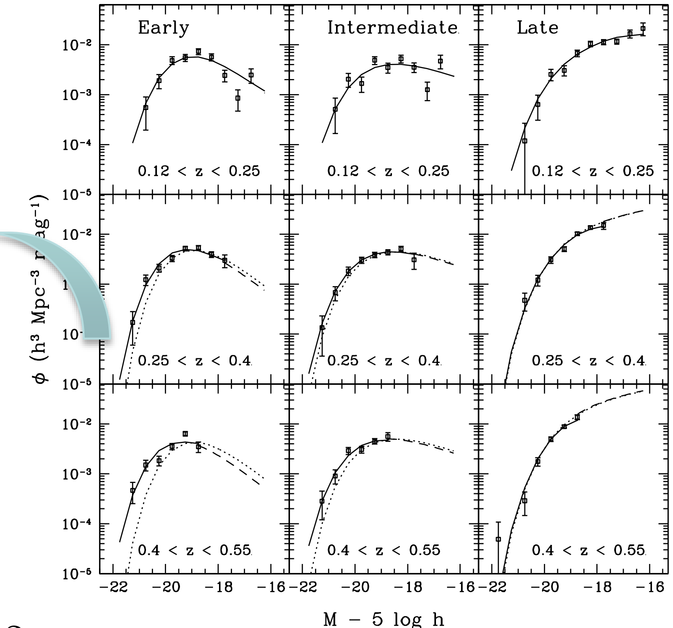

$$\Omega_{\mathrm{H\,I}} = \frac{\rho_{\mathrm{H\,I}}}{\rho_{\mathrm{crit}}}, \quad \rho_{\mathrm{crit}} = \frac{3H_0^2}{8\pi G},$$

Sample	z ~ 0.1					z ~ 0.2				
	N_{gal}	$\langle M_{\mathrm{H\,I}} \rangle$	$\langle L_B \rangle$	ρ_{L_B}	$\rho_{\mathrm{H\,I}}$	N_{gal}	$\langle M_{\mathrm{H\,I}} \rangle$	$\langle L_B \rangle$	ρ_{L_B}	$\rho_{\mathrm{H\,I}}$
Early	8	1.18 ± 0.39	7.85	6.45 ± 1.12	0.79 ± 0.30	25	0.13 ± 0.46	16.35	6.48 ± 1.35	0.05 ± 0.18
Intermediate	17	3.11 ± 0.45	14.13	4.42 ± 0.88	1.03 ± 0.25	25	1.94 ± 0.52	13.29	4.93 ± 1.26	0.71 ± 0.26
Late	34	1.43 ± 0.20	4.41	6.09 ± 1.19	2.61 ± 0.63	46	2.61 ± 0.35	9.15	7.90 ± 2.18	3.81 ± 1.16
All	$\Omega_{\mathrm{H\,I}}(z \sim 0.1) = (0.33 \pm 0.05) \times 10^{-3}$					$\Omega_{\mathrm{H\,I}}(z \sim 0.2) = (0.34 \pm 0.09) \times 10^{-3}$				

Cosmic H I mass density (Ω_{HI})

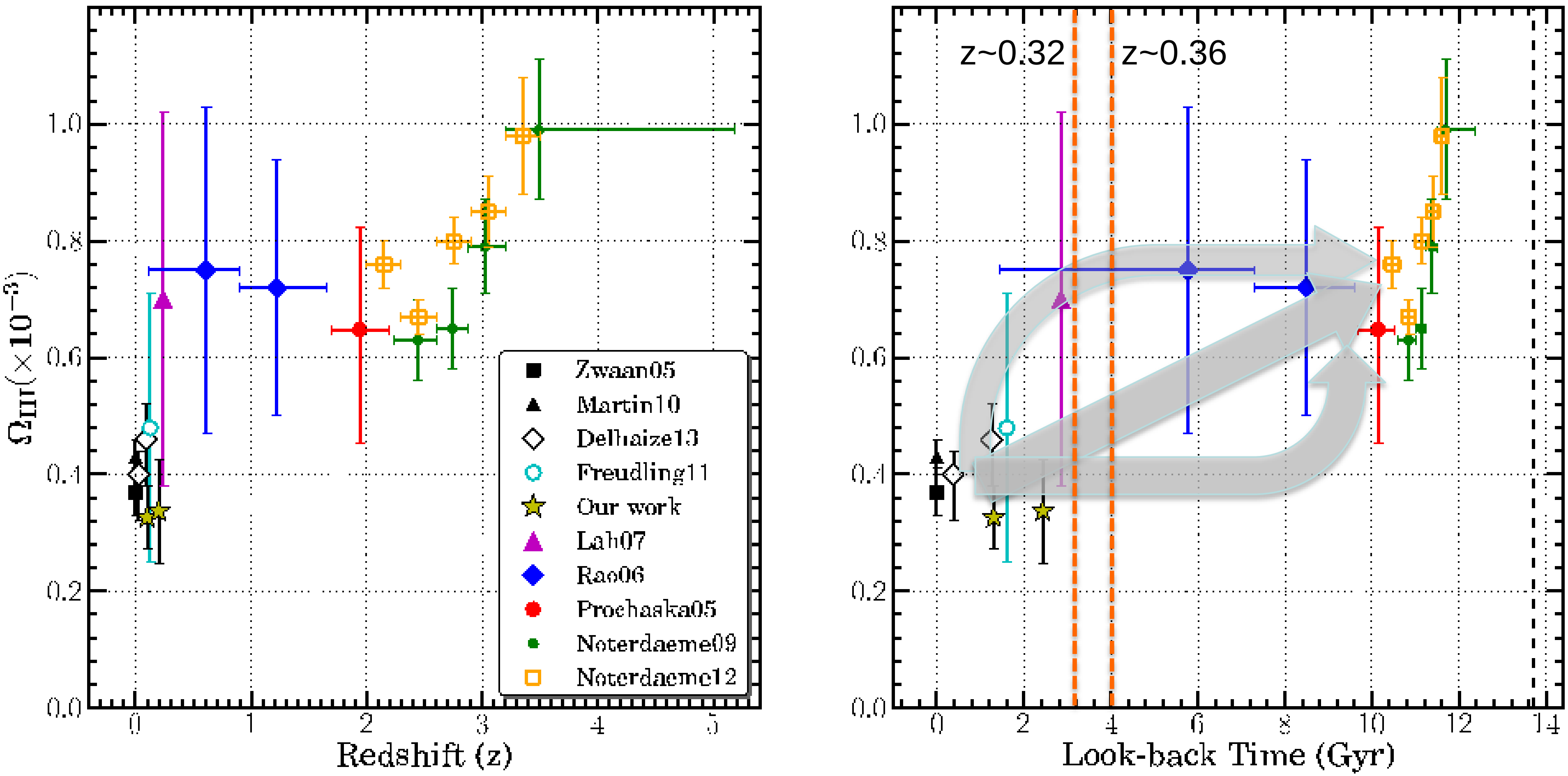

Conclusion

- The global H I abundance does not change significantly over last 2 Gyr (to z~0.2)
- Stacking technique works well at higher redshift
- H I spectral stacking is very useful for future H I surveys

Thank you

H I mass-to-light ratio ($M_{\rm HI}/L_B$)

Sample	$z \sim 0.1$ $\langle M_{\rm H\,I}\rangle/\langle L_B\rangle$	$z \sim 0.2$ $\langle M_{\rm H\,I}\rangle/\langle L_B\rangle$
Early	0.15 ± 0.05	0.01 ± 0.03
Intermediate	0.22 ± 0.03	0.15 ± 0.04
Late	0.32 ± 0.04	0.29 ± 0.04